Proc. Natl. Acad. Sci. USA
Vol. 87, pp. 9467–9471, December 1990
Biophysics

Oscillations and chaos in neural networks: An exactly solvable model

(bifurcation/noise/interference/associative memory/pattern recognition)

LIPO WANG, ELGAR E. PICHLER, AND JOHN ROSS*

Department of Chemistry, Stanford University, Stanford, CA 94305

Contributed by John Ross, September 10, 1990

ABSTRACT **We consider a randomly diluted higher-order network with noise, consisting of McCulloch–Pitts neurons that interact by Hebbian-type connections. For this model, exact dynamical equations are derived and solved for both parallel and random sequential updating algorithms. For parallel dynamics, we find a rich spectrum of different behaviors including static retrieving and oscillatory and chaotic phenomena in different parts of the parameter space. The bifurcation parameters include first- and second-order neuronal interaction coefficients and a rescaled noise level, which represents the combined effects of the random synaptic dilution, interference between stored patterns, and additional background noise. We show that a marked difference in terms of the occurrence of oscillations or chaos exists between neural networks with parallel and random sequential dynamics.**

Oscillations and chaos have been the subject of extensive studies in many chemical, physical, and biological systems. The Belousov–Zhabotinsky reaction (1), Rayleigh–Benard convection (2), and glycolysis (3) are well known examples.

Oscillatory phenomena frequently occur in living systems; some of these are a result of rhythmic excitations of the corresponding neural systems (e.g., locomotion, respiration, and heart beat). Recently, oscillations and chaos in neural networks have become the focus of a number of research efforts (4–19). Oscillations can occur in a neural system due to properties of single neurons (4–7, 20) and properties of synaptic connectivities among neurons (8–18) (for recent reviews on neural networks, see, e.g., refs. 21 and 22).

Single neurons with periodic forcing and delays in feedback have been studied (4) and oscillations and chaos have been found (for a review on oscillations in biological membranes, see ref. 20). Experimental observations have been made on the Onchidium pacemaker neuron and transition to chaos by intermittency has been pointed out (5). Both Hodgkin–Huxley-type (6) and Eyring multibarrier rate (7) theories for oscillatory behavior have been developed for single neurons.

The studies on oscillations in neural networks, originating from synaptic connectivities among neurons, may be further separated into the following two categories: (*i*) special geometries of neural network architecture that promote oscillations and (*ii*) delays in neural information transmissions. In category *i*, Derrida and Meir (8) studied chaotic behavior of a layered feed-forward neural network. Chaos has also been found in a neural network with completely random connectivity among neurons (9); however, no information (patterns) can be stored in this system. Other geometries that promote oscillations include ring-like (with closed loops) neural networks (10) and a network with both random synapses and random firing thresholds (11). Category *ii* includes natural or imposed delays that may also result in oscillations and chaos in neural networks (12, 13), as they do in many physical and chemical systems (23). Oscillations can also occur in temporal sequence retrieving that can be achieved through delays (14–16) and time-dependent synaptic connections (17, 18).

In this paper we present a model closer to standard neural network theory, one based on the work of Derrida *et al.* (24). Our neural network model can however, unlike their model, display oscillations and chaos. In this approach, we study a higher-order neural network that consists of simple McCulloch–Pitts neurons (25); the connections in the network are defined by a modified Hebb learning rule. Both first- and second-order synapses are disconnected randomly at one time to model the observed incomplete connectivity in real neural systems; thereby, we derive exact solutions of the network dynamics. Two updating algorithms are considered: random sequential updating and synchronous updating. We show that the network can exhibit a variety of dynamical behaviors such as stable retrieving, oscillations, and chaos. A difference between asynchronously and synchronously updated neural networks exists inasmuch as the occurence and the size of oscillatory and chaotic attractors depend on the size of the network for randomly updated neural networks and are independent of the size in the synchronous case. We show that a rescaled noise level that represents the combined effects of the random synaptic dilution, interference between stored patterns, and additional background noise acts as an important bifurcation parameter in the present system.

FORMULATION

We consider N McCulloch–Pitts neurons (25) that have two states (i.e., $S_i = \pm 1$) and are connected by both first-order and second-order Hebbian-type connections. Suppose that the total input for the ith neuron is (26, 27)

$$h_i(t) = \gamma_1 \sum_{j=1}^{N} T_{ij} S_j(t) + \gamma_2 \sum_{j,k=1}^{N} T_{ijk} S_j(t) S_k(t) + \eta_i, \quad [1]$$

where $S_j(t)$ represents the state of the jth neuron at time t,

$$T_{ij} = \frac{C_{ij}}{N} \sum_{\mu=1}^{p} S_i^\mu S_j^\mu \text{ and } T_{ijk} = \frac{C_{ijk}}{N} \sum_{\mu=1}^{p} S_i^\mu S_j^\mu S_k^\mu, \quad [2]$$

are the modified Hebbian synaptic efficacies (26–30), $\vec{S}^\mu$ is the μth stored pattern, and p is the number of patterns stored. Coefficients γ_1 and γ_2 measure the relative strengths of first-order and second-order interactions (for experimental evidence of nonlinear multiplicative neuronal interactions, see, e.g., refs. 31–33). We have introduced random asymmetric dilution in the efficacies T_{ij} and T_{ijk} by choosing random variables C_{ij} and C_{ijk} according to the following distributions:

$$\rho(C_{ij}) = \frac{C}{N} \delta(C_{ij} - 1) + \left(1 - \frac{C}{N}\right) \delta(C_{ij}), \quad [3]$$

The publication costs of this article were defrayed in part by page charge payment. This article must therefore be hereby marked "*advertisement*" in accordance with 18 U.S.C. §1734 solely to indicate this fact.

*To whom reprint requests should be addressed.

and

$$\rho(C_{ijk}) = \frac{2C}{N^2}\,\delta(C_{ijk} - 1) + \left(1 - \frac{2C}{N^2}\right)\delta(C_{ijk}). \qquad [4]$$

Eq. **3** was first used by Derrida *et al.* (24) in their discussion of a first-order diluted network. Synaptic dilution is essential in modeling the observed incomplete connectivity in real neurophysiological systems and for the possibility of assuring an exact solution (24). We generalize their work to include higher-order interactions. We include a background random Gaussian noise η_i with a standard deviation σ_0 in Eq. **1** to account for the presence of noise (temperature). Noise in neurophysiological systems may be attributed to spontaneous neural firing and statistical variation of the number of vesicles containing neurotransmitters (e.g., acetylcholine) released at the synaptic junctions (34–37) (for experimental evidence that supports a Gaussian noise distribution, see, e.g., page 21 of ref. 36). In artificial implementations of neural networks (38–42), noise may result from electrical, thermal, and quantum fluctuations.

The updating rule is

$$S_i(t + \Delta t) = \text{sign}[h_i(t)], \qquad [5]$$

where $\text{sign}(x) = -1$ for negative x and $\text{sign}(x) = +1$ for positive x. We consider the following two dynamics: parallel and random sequential dynamics. In parallel dynamics, all neurons are updated simultaneously and $\Delta t = 1$. In random sequential dynamics, one neuron among the N neurons is chosen at random at time t and this neuron is updated according to Eq. **5**; $\Delta t = 1/N$ for random updating to ensure that the same number of neurons is updated per time step in the parallel mode and in the sequential mode.

Suppose that the initial state of the network is set in the neighborhood of pattern $\vec{S}^1$. Explicitly, we let

$$m^1(0) = \max\{m^\mu(0) | \mu = 1, 2, \ldots, p\}, \qquad [6]$$

where

$$m^\mu(t) = \frac{1}{N}\vec{S}^\mu \cdot \vec{S}(t) \qquad [7]$$

is the overlap between the state of the system at time t and the μth pattern.

Consider the ith neuron and let $j_1, j_2, \ldots, j_{K_1}$ be the K_1 neurons j such that $T_{ij} \neq 0$. Let $j_1k_1, j_2k_2, \ldots, j_{K_2}k_{K_2}$ be the K_2 pairs of neurons $\{jk\}$ such that $T_{ijk} \neq 0$. These choices of notation do not imply that, for a given j', if $T_{ij'} \neq 0$, then $T_{ij'k} \neq 0$, since dilutions of first- and second-order interactions are independent of each other. According to Eqs. **3** and **4**, the averages of K_1 and K_2 are both C, compared with fully connected networks where the numbers of first-order and second-order synaptic connections are on the orders of N and $N(N + 1)/2 \doteq N^2/2$ (for large N), respectively.

We separate the first two terms in the total signal (Eq. **1**) into two parts (24, 27, 43):

$$h_i(t) = \left\{\frac{\gamma_1}{N}\sum_{r=1}^{K_1} m^1_{j_r}(t) + \frac{\gamma_2}{N}\sum_{r=1}^{K_2} m^1_{j_r}(t)m^1_{k_r}(t)\right\}S^1_i + \left\{\frac{\gamma_1}{N}\sum_{\mu=2}^{p}\sum_{r=1}^{K_1} S^\mu_i S^\mu_{j_r} S_{j_r}(t) + \frac{\gamma_2}{N}\sum_{\mu=2}^{p}\sum_{r=1}^{K_2} S^\mu_i S^\mu_{j_r} S^\mu_{k_r} S_{j_r}(t) S_{k_r}(t)\right\}; \qquad [8]$$

where

$$m^1_q(t) = S^1_q S^1_q(t). \qquad [9]$$

The first term in Eq. **8** is proportional to the overlap of the system with pattern $\vec{S}^1$. The second part consists of interferences from patterns $\vec{S}^2, \vec{S}^3, \ldots, \vec{S}^p$. As shown by a number of authors for a first-order interaction ($\gamma_2 = 0$) (24, 44–46), the correlations between neurons can be neglected in the limit of extreme dilution. We now prove that this result holds in the presence of both diluted first- and second-order interactions, as given by Eqs. **2–4**. The calculation of the state of the ith neuron at time t [i.e., $S_i(t)$] involves a tree of ancestors (states of neurons at previous time steps) that connects the ith neuron to the initial conditions at time $t = 0$ (24), where t is the time required for the network to reach equilibrium. At each time step the state of the ith neuron is influenced by about C neurons through first-order interactions and $2C$ (C pairs) neurons through second-order interactions, and the number of neurons in this tree is typically less than $(3C)^t$. Thus as long as $C << \ln N$, almost all neurons in this tree are different [i.e., $(3C)^t << N$], since $\ln N << N^{1/t}$ for large N. So, in this diluted limit, the states in Eq. **8** $S_{j_1}, \ldots, S_{j_{K_1}}, \ldots, S_{k_{K_2}}$ are uncorrelated. According to the central limit theorem, the interference terms are random and Gaussian, distributed with a total average of zero and a total squared deviation

$$\sigma^2_{ct} \equiv (p - 1)[\gamma_1^2 K_1/N^2 + \gamma_2^2 K_2/N^2] \qquad [10]$$

in the limit of large N. Furthermore, when we average over all shapes of the tree of ancestors, all the $m^1_q(t)$ given by Eq. **9** have the same average $m(t)$ (24). It follows from Eqs. **5** and **7–9** that for parallel dynamics

$$m(t + 1) = \frac{1}{N}\sum_{i=1}^{N} S_i \text{sign}\left\{\left[\gamma_1\left(\frac{C}{N}\right)m(t) + \gamma_2\left(\frac{C}{N}\right)[m(t)]^2\right]S_i + \eta'\right\}. \qquad [11]$$

In Eq. **11**, η' is the combination of the internal noise η_i and the interference terms and the standard deviation of η' is $\sigma_{\text{total}} = (\sigma^2_{ct} + \sigma^2_0)^{1/2}$ (27), where K_1 and K_2 in Eq. **10** have been replaced by their averages C. We have omitted superscript "1" in Eq. **11**; we refer to the overlap between the state of the system with pattern $\vec{S}^1$, unless specified otherwise. Considering the fact that η' is a Gaussian and the value of S_i can be either -1 or $+1$, we obtain the dynamical equation for the parallel updating algorithm in the present model

$$m(t + 1) = 1 - 2\psi\{\gamma_1 m(t) + \gamma_2[m(t)]^2\} \equiv F[m(t), \sigma] \qquad [12]$$

with

$$\psi(y) = \frac{1}{\sqrt{2\pi}}\int_{y/\sigma}^{+\infty} e^{-x^2/2}dx, \qquad [13]$$

and a rescaled noise deviation:

$$\sigma \equiv \sqrt{(\gamma_1^2 + \gamma_2^2)[(p - 1)/C] + (\sigma_0 N/C)^2}. \qquad [14]$$

In Eqs. **3** and **4**, we have used the same dilution constant C for both the first- and the second-order interactions. If one uses different dilution constants, the resulting effects can be absorbed into coefficients γ_1 and γ_2 (see Eq. **10**). Hence no generality has been lost by choosing the same dilution constant C for all orders of interactions.

For random sequential updating, we select at random a neuron to update at time t so that we have from Eqs. **5**, **7**, and **12**:

$$m\left(t+\frac{1}{N}\right)=\frac{N-1}{N}m(t)+\frac{1}{N}m\left(t+\frac{1}{N}\right)$$

$$=m(t)+\frac{1}{N}\{F[m(t),\sigma]-m(t)\}. \quad [15]$$

We see (47) that the mapping function, Eq. **15**, is bounded by $m(t) - 1/N[m(t) \pm 1]$ since $0 \le \psi[m(t), \sigma] \le 1$. It is obvious that the bounding region for $m(t + 1/N)$ grows as N decreases. It is also evident from Eqs. **12** and **15** that the fixed points of the dynamical equations for parallel and sequential updating are the same. But, considering the derivative of Eq. **15** with respect to m, we see that the stability of a fixed point for random sequential dynamics depends on the size of the system, whereas size does not have any effect on the stability of a solution for parallel dynamics. Furthermore, unstable fixed points of Eq. **15** may have corresponding attractors (limit cycles, chaotic attractors) that cannot be larger than $2/N$. $|\Delta m| = 2/N$ for two sequences with Hamming distances d and $d + 1$ from the reference pattern $\vec{S}^1$. Therefore, these attractors span, at the maximum, two sets of states: (*i*) the difference of Hamming distances between states in one set and the reference pattern (*ii*) and states in the other set and the reference pattern is one. Periodic orbits of order higher than one for random sequential dynamics (of large systems) are, therefore, expected to be of theoretical interest only. In the limit $N \to \infty$, the attractors are infinitely small for a sequentially updated network and the dynamics are described by the differential equation

$$\frac{dm(t)}{dt}=F[m(t),\sigma]-m(t). \quad [16]$$

RESULTS AND DISCUSSION

Eqs. **12–16** are a generalization of the formulation of Derrida *et al.* (24), who derived an exact solution of a diluted neural network with first-order interactions only for which neither oscillations nor chaos are possible. Furthermore, they used Little's definition of temperature (48) instead of the Gaussian noise used in the present work.

Eqs. **12** and **13** have been derived first by Keeler *et al.* (27) for a fully connected network by the approximation that the interference is random Gaussian noise in the absence of dilution. They have found that compared to the case with only first-order interaction ($\gamma_1 = 1$, $\gamma_2 = 0$), the final retrieval ability is enhanced by letting $\gamma_1 = 1$, $\gamma_2 > 0$, which we call the "positive" second-order interaction. The "positive" second-order interaction also causes hysteresis in the retrieval-noise curves (27). We show that the formulation of Keeler *et al.* (27) becomes exact in the diluted limit.

In the present paper, we show that the system exhibits, under certain conditions, a variety of dynamical phenomena, such as oscillations, period doubling bifurcations, chaos, as well as stable retrievals if second-order interactions exist. We show this for $\gamma_1 > 0$, $\gamma_2 < 0$, which we call the "negative" second-order interaction.

Let us first consider parallel dynamics. The equation of motion of the neural network is given by Eq. **12**, which is a one-dimensional map (49) of the overlap between the state of the network and the stored pattern $\vec{S}^1$, $m(t)$, with three parameters: first-order and second-order interaction coefficients, γ_1 and γ_2, and the rescaled noise level σ given by Eq. **14**, which includes the effects of random synaptic dilution, interference between stored patterns, and additional background noise. Some general conclusions may be drawn from Eqs. **12** and **13**. First of all, there is no nonnegative fixed point if $\gamma_1 = 0$. We assume that $\gamma_1 \neq 0$ from now on. Eqs. **12** and **13** show that a network with parameters γ_1, γ_2, and σ are equivalent to a network with $\gamma_1' = 1$, $\gamma_2' = \gamma_2/\gamma_1$, and $\sigma' = \sigma/\gamma_1$. Hence we choose $\gamma_1 = 1$ without loss of generality. The fixed points of the system can be obtained by iterating Eq. **12** for many time steps.

We now consider the case $\gamma_2 = -1$ where the solutions of $m \equiv m(t = \infty)$ as a function of the noise level σ are presented in Fig. 1.

When $\sigma > \sqrt{2/\pi} = 0.798$, the only nonnegative fixed points are zeros. For $\sqrt{2/\pi} = 0.798 > \sigma > 0.193$, the system converges to a single branch of stable positive fixed points with any positive initial overlap. As the noise level decreases below $\sigma_1 = 0.193$, oscillations start to appear. As shown in Fig. 1, there is a complete period-doubling sequence between $\sigma_1 = 0.193$ and $\sigma_\infty = 0.1234$, which is the saturation point of that sequence. Space-filling chaotic structures and periodic windows can be seen beyond this saturation point. Period 6, period 5, and period 3 windows are marked in Fig. 1. Period 3 implies chaos (42). The order of occurrence of these stable periodic orbits is predicted by the Sarkovskii sequence (page 169 of ref. 49). Around the periodic windows there are the typical chaotic "explosions": space-filling bands appear abruptly at certain points of bifurcation.

As γ_2 is increased above -1, bifurcations become incomplete (page 172 of ref. 49) in the sense that the oscillatory region is smoothly connected with stable fixed points on both sides, as shown in Fig. 2 where $\gamma_2 = -0.99$. As γ_2 is further increased, oscillatory and chaotic dynamics rapidly disappear, with more complex structures diminishing first. For $\gamma_2 = -0.8$, for instance, the only type of oscillation the system exhibits has a period of 2. Stable fixed points become the only attractors of the system when $\gamma_2 > -0.87$. For $\gamma_2 < -1$, however, the positive oscillatory attractors abruptly disappear at certain low noise level, which is often called "crisis," as shown in Fig. 3 for $\gamma_2 = -2$. The solid line marked with the arrow in Fig. 3 represents the stable negative fixed points.

The network dynamics described above can be understood through the mapping function given by Eqs. **12** and **13**. Curves a through f in Fig. 4 are plots of the mapping $F(m,\sigma)$ vs. the overlap m, for different values of σ and γ_2. As long as $\gamma_2 < 0$, there are positive maxima for each noise level σ, which is the origin of the oscillatory and chaotic structures in the system. For instance, for $\gamma_2 = -1$ (curves a and b), as the

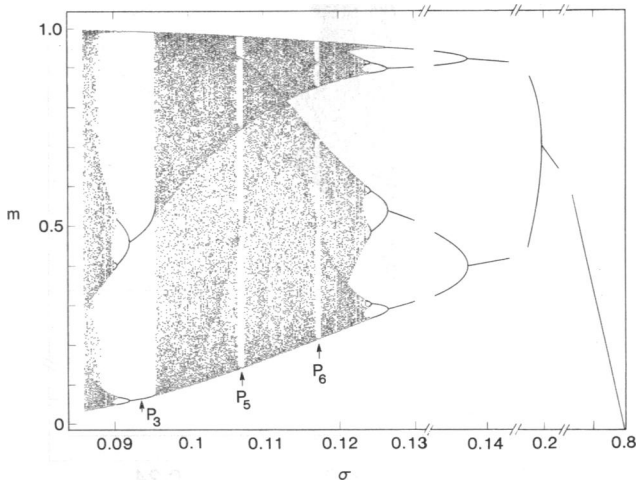

FIG. 1. Fixed points for parallel updating (according to Eq. **12**) vs. standard deviation of the Gaussian noise σ, with $\gamma_1 = 1$ and $\gamma_2 = -1$.

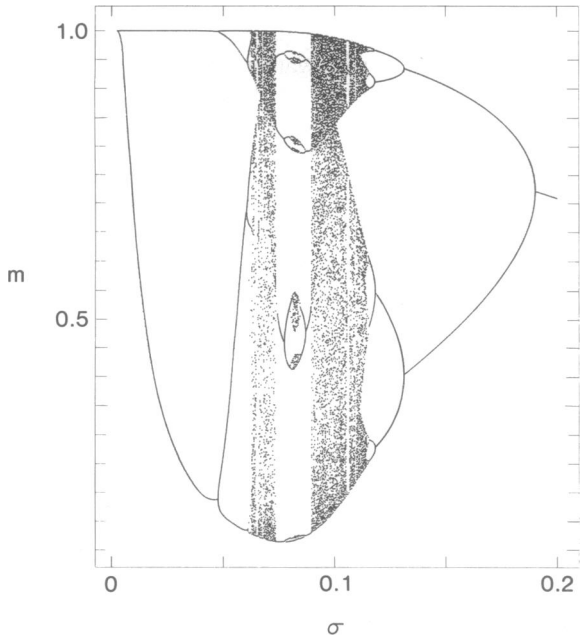

FIG. 2. Same as in Fig. 1, with $\gamma_1 = 1$ and $\gamma_2 = -0.99$.

noise level σ is reduced below the critical value 0.798, there is one intersecting point, other than the origin, with positive overlap m, between the mapping function and the diagonal straight line. In curve a, $\sigma = 0.5$ and the slope at the intersecting point is greater than -1. Hence the intersecting point represents a stable fixed point (49). As σ is reduced further, the first Hopf bifurcation to oscillations occurs when $\sigma_1 = 0.193$ (curve b) and the slope at the intersecting point between the mapping function and the diagonal line (referred as "the slope" thereafter) is -1. The slope decreases (becomes more negative) monotonically as σ decreases and more complex oscillations appear (see Fig. 1).

From Eqs. **12** and **13**, we observe the following general properties of the mapping function F. For each σ, F has two zeros: F always equals 0 when $m = 0$, and the second zero is at $m = -1/\gamma_2$. For each γ_2, the mapping function F reaches its positive maximum for each σ when $m = -1/(2\gamma_2)$. For

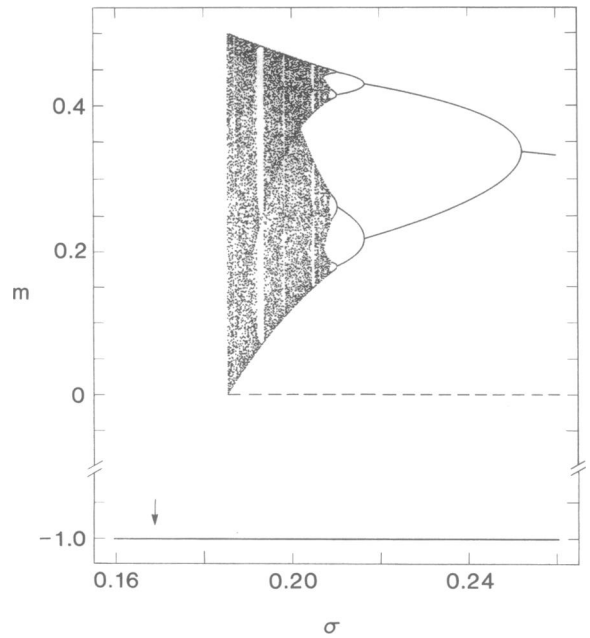

FIG. 3. Same as in Fig. 1, with $\gamma_1 = 1$ and $\gamma_2 = -2$.

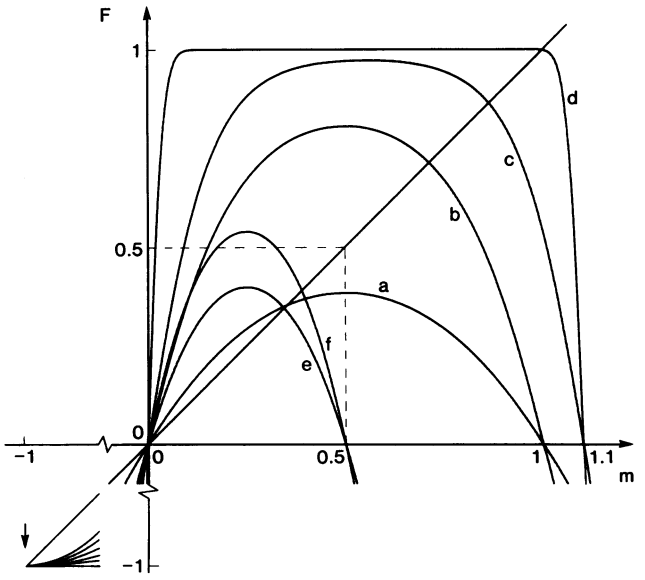

FIG. 4. Mapping function F given by Eqs. **12** and **13** vs. m for different noise levels σ and second-order interaction coefficients γ_2. Curves: a, $\gamma_2 = -1$, $\sigma = 0.5$ (stable fixed point); b, $\gamma_2 = -1$, $\sigma = 0.193$ (Hopf bifurcation); c, $\gamma_2 = -0.91$, $\sigma = 0.125$ (period 2 oscillation); d, $\gamma_2 = -0.91$, $\sigma = 0.03$ (stable fixed point); e, $\gamma_2 = -2$, $\sigma = 0.24$ (period 2 oscillation); f, $\gamma_2 = -2$, $\sigma = 0.17$ (crisis).

each m and γ_2, F increases monotonically as σ decreases. F approaches 1 as σ approaches 0 for all γ_2 and $0 < m < -1/\gamma_2$. Hence for $\gamma_2 < -1$ and small enough σ values, the positive maximum of the mapping is above (outside) the square box (curve f, with $\gamma_2 = -2$ and $\sigma = 0.17$). A trajectory initially inside the box eventually goes out of it after some iterations and is attracted to the stable negative fixed point (marked by the arrow in Fig. 4), which is the reason for crisis to occur as shown in Fig. 3 (abrupt disappearance of positive attractors below certain noise level). In curve e, $\gamma_2 = -2$ and $\sigma = 0.24$, the mapping function is contained in the box and the slope is less than -1, which corresponds to a period 2 oscillation in

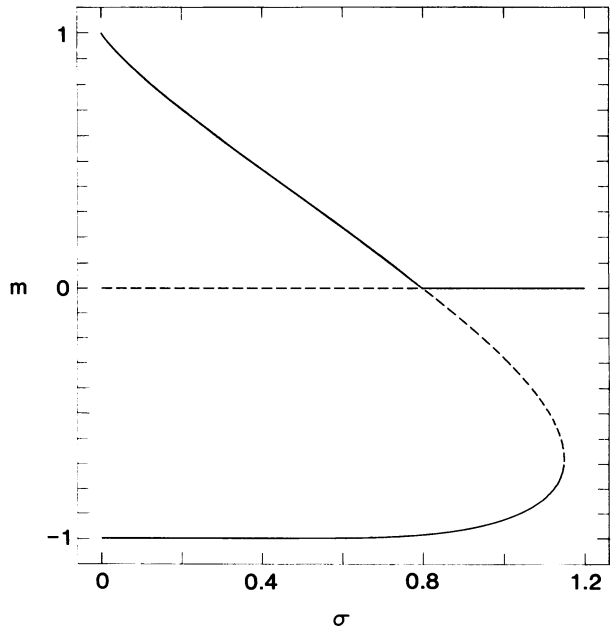

FIG. 5. Fixed points for random sequential updating (according to Eq. **16**) vs. standard deviation of the Gaussian noise σ, with $\gamma_1 = 1$ and $\gamma_2 = -1$. Dashed portions are unstable.

Fig. 3. We note that the first Hopf bifurcation appears at a higher noise level σ_1 for a more negative γ_2 (e.g., $\sigma_1 = 0.252$ for $\gamma_2 = -2$, compared with $\sigma_1 = 0.193$ for $\gamma_2 = -1$).

For $-0.87 > \gamma_2 > -1$, oscillations still exist for some noise levels. Since the slope does not decrease monotonically as σ decreases, mappings result in incomplete bifurcations (page 172 of ref. 49; also see Fig. 2). For instance, in curve c, $\gamma_2 = -0.91$ and $\sigma = 0.125$, the slope is less than -1 and corresponds to a period 2 oscillation. As σ decreases further, the slope increases above -1 and the oscillation diminishes (see curve d, with $\sigma = 0.03$ and $\gamma_2 = -0.91$). For $\gamma_2 > -0.87$, the mapping results only in stable fixed points for all σ, since the slope never falls below -1.

Eq. **16** describes the dynamics of random sequential updating. It is well known that a one-dimensional system described by a differential equation cannot exhibit oscillatory behavior. Hence the random sequential dynamics given by Eq. **16** have only two types of nonoscillatory fixed points, either stable or unstable. The result for $\gamma_2 = -1$ is given in Fig. 5. The unstable fixed points shown by dashed lines represent the boundaries of basins of attractions of the stable fixed points (solid lines).

We thank Igor Schreiber for numerous stimulating discussions. This work was supported in part by the National Science Foundation.

1. Field, R. J. & Burger, M. (1984) *Oscillations and Traveling Waves in Chemical Systems* (Wiley, New York).
2. Behringer, R. P. (1985) *Rev. Mod. Phys.* **57,** 657–687.
3. Hess, B. & Boiteux, A. (1971) *Annu. Rev. Biochem.* **40,** 237–258.
4. Guevara, M. R., Glass, L., Mackey, M. C. & Shrier, A. (1983) *IEEE Trans. Syst. Man. Cybern.* **13,** 790–798.
5. Hayashi, H., Ishizuuka, S. & Hirakawa, K. (1983) *Phys. Lett.* **98A,** 474–476.
6. Rinzel, J. & Miller, R. N. (1980) *Math. Biosci.* **49,** 27–59.
7. Chay, T. R. (1983) *J. Phys. Chem.* **87,** 2935–2940.
8. Derrida, B. & Meir, R. (1988) *Phys. Rev. A* **38,** 3116–3119.
9. Sompolinsky, H., Crisanti, A. & Sommers, H. J. (1988) *Phys. Rev. Lett.* **61,** 259–262.
10. Tsutsumi, K. & Matsumoto, H. (1984) *Biol. Cybern.* **50,** 419–430.
11. Amari, S.-I. (1971) *Proc. IEEE* **59,** 35–46.
12. Conwell, P. R. (1987) *Proc. IEEE First Int. Conf. Neural Networks*, San Diego, pp. III-96–104.
13. Marcus, C. M. & Westervelt, R. M. (1989) *Phys. Rev. A* **39,** 347–359.
14. Sompolinsky, H. & Kanter, I. (1986) *Phys. Rev. Lett.* **57,** 2861–2864.
15. Kleinfeld, D. (1986) *Proc. Natl. Acad. Sci. USA* **83,** 9469–9473.
16. Riedel, U., Kühn, R. & van Hemmen, J. L. (1988) *Phys. Rev. A* **38,** 1105–1108.
17. Shaw, G. L., Silverman, D. J. & Pearson, J. C. (1985) *Proc. Natl. Acad. Sci. USA* **82,** 2364–2368.
18. Tsuda, I., Koerner, E. & Shimizu, H. (1987) *Prog. Theor. Phys.* **78,** 51–71.
19. Skarda, C. A. & Freeman, W. J. (1987) *Behav. Brain Sci.* **10,** 161–195.
20. Larter, R. (1990) *Chem. Rev.* **90,** 355–381.
21. Crick, F. (1989) *Nature (London)* **337,** 129–132.
22. Sompolinsky, H. (1988) *Phys. Today* **41,** 70–80.
23. Ross, J., Pugh, S. & Schell, M. (1988) in *From Chemical to Biological Organization*, eds. Markus, M., Müller, S. C. & Nicolis, G. (Springer, Berlin), pp. 34–46.
24. Derrida, B., Gardner, E. & Zippelius, A. (1987) *Europhys. Lett.* **4,** 167–173.
25. McCulloch, W. S. & Pitts, W. (1943) *Bull. Math. Biophys.* **5,** 115–133.
26. Peretto, P. & Niez, J. J. (1986) *Biol. Cybern.* **54,** 53–63.
27. Keeler, J. D., Pichler, E. E. & Ross, J. (1989) *Proc. Natl. Acad. Sci. USA* **86,** 1712–1716.
28. Cooper, L. N., Liberman, F. & Oja, E. (1979) *Biol. Cybern.* **33,** 9–28.
29. Kürten, K. E. (1990) in *Parallel Processing in Neural Systems and Computers*, eds. Eckmiller, R., Hartmann, G. & Hauske, G. (Elsevier–North-Holland, Amsterdam), pp. 191–194.
30. Hebb, D. O. (1949) *The Organization of Behavior* (Wiley, New York), p. 44.
31. Kandel, E. R. & Tauc, L. (1965) *J. Physiol. (London)* **181,** 1–27.
32. Roney, K. J., Scheibel, A. B. & Shaw, G. L. (1979) *Brain Res. Rev.* **1,** 225–271.
33. Shaw, G. L., Harth, E. & Scheibel, A. B. (1982) *Exp. Neurol.* **77,** 324–358.
34. Shaw, G. L. & Vasudevan, R. (1974) *Math. Biosci.* **21,** 207–218.
35. Sejnowski, T. J. (1981) in *Parallel Models of Associative Memory*, eds. Hinton, G. & Anderson, J. (Lawrence Erlbaum Associates, Hillsdale, NJ), pp. 189–212.
36. Abeles, M. (1982) *Local Cortical Circuits* (Springer, New York).
37. Carpenter, R. H. S. (1984) *Neurophysiology* (University Park Press, Baltimore, MD).
38. Jackel, L. D., Howard, R. E., Graf, H. P., Straughn, B. & Denker, J. S. (1986) *J. Vac. Sci. Technol.* **B4,** 61–63.
39. Farhat, N. H., Psaltis, D., Prata, A. & Paek, E. (1985) *Appl. Opt.* **24,** 1469–1475.
40. Psaltis, D. & Farhat, N. H. (1985) *Opt. Lett.* **10,** 98–100.
41. Psaltis, D., Park, C. H. & Hong, J. (1988) *Neural Networks* **1,** 149–163.
42. Li, T. Y. & Yorke, J. A. (1975) *Am. Math. Monthly* **82,** 985–992.
43. Kinzel, W. (1985) *Z. Phys.* **B60,** 205–213.
44. Derrida, B. & Weisbuch, G. (1986) *J. Phys. (Paris)* **47,** 1297–1303.
45. Derrida, B. & Pomeau, Y. (1986) *Europhys. Lett.* **1,** 45–49.
46. Hilhorst, H. J. & Nijmijer, M. (1987) *J. Phys. (Paris)* **48,** 185–191.
47. Pichler, E. (1990) *Ph.D. Thesis* (University of Vienna).
48. Little, W. A. (1974) *Math. Biosci.* **19,** 101–120.
49. Thompson, J. M. T. & Stewart, H. B. (1986) *Nonlinear Dynamics and Chaos* (Wiley, New York).